JACS
JOURNAL OF THE AMERICAN CHEMICAL SOCIETY
pubs.acs.org/JACS
Article

From Photoinduced Supramolecular Polymerization to Responsive Organogels

Fan Xu, Lukas Pfeifer, Stefano Crespi, Franco King-Chi Leung, Marc C. A. Stuart, Sander J. Wezenberg, and Ben L. Feringa*

Cite This: J. Am. Chem. Soc. 2021, 143, 5990−5997
Read Online
ACCESS | Metrics & More | Article Recommendations | Supporting Information

ABSTRACT: Controlling supramolecular polymerization by external stimuli holds great potential toward the development of responsive soft materials and manipulating self-assembly at the nanoscale. Photochemical switching offers the prospect of regulating the structure and properties of systems in a noninvasive and reversible manner with spatial and temporal control. In addition, this approach will enhance our understanding of supramolecular polymerization mechanisms; however, the control of molecular assembly by light remains challenging. Here we present photoresponsive stiff-stilbene-based bis-urea monomers whose *trans* isomers readily form supramolecular polymers in a wide range of organic solvents, enabling fast light-triggered depolymerization−polymerization and reversible gel formation. Due to the stability of the *cis* isomers and the high photostationary states (PSS) of the *cis*−*trans* isomerization, precise control over supramolecular polymerization and *in situ* gelation could be achieved with short response times. A detailed study on the temperature-dependent and photoinduced supramolecular polymerization in organic solvents revealed a kinetically controlled nucleation−elongation mechanism. By application of a Volta phase plate to enhance the phase-contrast method in cryo-EM, unprecedented for nonaqueous solutions, uniform nanofibers were observed in organic solvents.

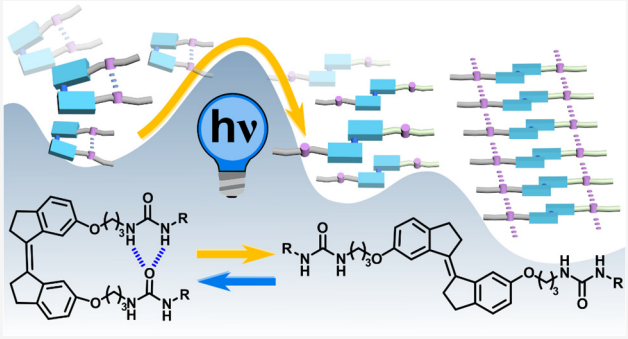

INTRODUCTION

As highly organized assemblies, supramolecular polymers play a distinct role in various areas of chemistry, biology, and materials science[1−10] and as functional systems including applications in responsive sensors,[7,9] electronic devices,[8] and biomedical materials.[5,10] They are also ideal candidates for the formation of supramolecular gels,[11−13] which hold great potential on the basis of their intricate properties,[14−17] such as chiral selection,[18] amplification,[19] and microactuation.[20,21] Elegant mathematical models have been developed for different types of polymerization mechanisms,[1−4] e.g. isodesmic,[22] cooperative,[23,24] and others,[25,26] revealing the dynamic and tunable nature of synthetic supramolecular systems and providing the tools for controlling their assembly processes.[27,28,67] Recent advances have focused on manipulating supramolecular polymerization by using external stimuli, e.g. ultrasound,[29,30] light,[31,32] and chemicals,[33,34] in order to develop responsive and adaptive materials.[5,7,10,35]

Among these stimuli, light has the distinct advantage of allowing the direct control of responsive materials through a noninvasive action with high spatiotemporal resolution.[36−40] One of the main approaches to realize reversibility in supramolecular assemblies exploits the photoisomerization of molecular switches,[41−45] such as azobenzenes[42,43,45] and dithienylethenes.[18,19,46] The majority of the recent studies on supramolecular assemblies have focused on the photoregulation of the responsive properties associated with the disassembly and reconfiguration of aggregates,[14−19] e.g. gel−sol transition,[42] volume,[43] and morphology[45] changes, while limited effort has been devoted to trigger the actual supramolecular polymerization step by using light.[31,32] Notably, Meijer and co-workers reported a cooperative polymerization, where a photoswitchable ligand regulated the fraction of stacked porphyrin monomers.[31] Subsequently, Takeuchi et al. demonstrated a photoregulated living supramolecular polymerization by combining polymerization and photoisomerization of azobenzene derivatives, in which the activation of the monomer was achieved by *cis* to *trans* photoisomerization or thermal reversion.[32] However, control of the macroscopic properties of these supramolecular polymers was not discussed, and these photoinduced supra-

Received: February 15, 2021
Published: April 8, 2021

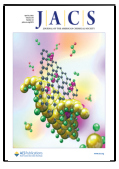

https://doi.org/10.1021/jacs.1c01802
J. Am. Chem. Soc. 2021, 143, 5990−5997

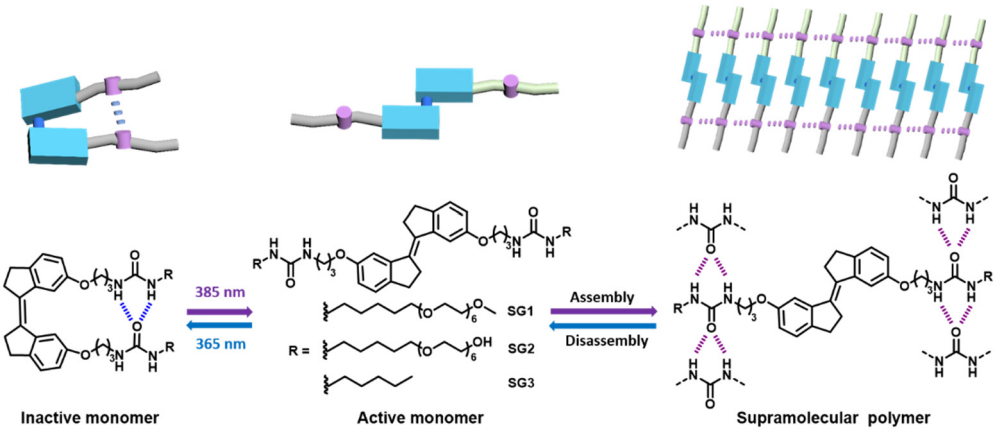

Figure 1. Schematic illustrations of the photoisomerization of SGs, the supramolecular polymerization of *trans*-**SG1**, and the process of the assembly and disassembly in organic solvents.

molecular polymerizations were based on azobenzene monomers[32] or ligands:[31] this photoswitch has the intrinsic disadvantage of *cis*−*trans* thermal back-isomerization, which limits the bistability of the system.

Here we report a light-controlled self-assembly process based on photoresponsive stiff-stilbene bis-urea monomers which form supramolecular polymers and responsive gels (Figure 1). Notably, the thermal isomerization between the *cis* and *trans* isomers of stiff-stilbene is negligible at room temperature due to the high energy barrier for interconversion.[44,47,48] This property offers the opportunity to design a robust bistable system in which supramolecular polymerization can be controlled by irradiation. A series of responsive monomers was obtained on the basis of the stiff-stilbene core bearing two symmetrical urea moieties with different end groups (**SG1**−**SG3**). According to the definition of Meijer et al.,[2,3] the obtained 1D assemblies qualify as supramolecular polymers. The outstanding ability of the urea groups to self-assemble has been demonstrated in previous studies by our group[38,49,50] and others.[51−53] In the present design, bis-ureas form intermolecular hydrogen bonds between the *trans* isomers, in contrast to the intramolecular hydrogen bond, formed when the molecule is in its *cis* form. On the basis of these different hydrogen-bonding patterns, starting from a *cis* isomer (inactive monomer), the polymerization only takes place after conversion to the *trans* isomer (active monomer). In other words, the active monomer can be "unlocked" from the dormant state upon irradiation. Hence, we could design a bistable supramolecular system benefiting from the high energy barrier between isomers and precisely control its assembly with light in a reversible manner (Figure 1). The mechanism of temperature-dependent polymerization was studied in detail in toluene. We further developed these supramolecular polymers to functional gels with photocontrolled sol−gel transitions.

RESULTS AND DISCUSSION

Molecular Design and Synthesis of SGs. The stiff-stilbene monomers were designed with a photoresponsive core bearing two urea groups, enabling intermolecular (*trans* isomers) and intramolecular hydrogen-bonding (*cis*-isomers, see Figure 1). Hexaethylene glycol and hexaethylene glycol methyl ether served as the end group of **SG1** and **SG2**, respectively, and were connected to the urea group through alkyl-linkers.[54−56] The detailed synthesis routes for *trans* and *cis* isomers of SGs are summarized in Figure S1, and pure *trans* isomers of **SG1**, **SG2**, and **SG3** as well as *cis*-**SG1** were obtained. All of the novel structures were confirmed unambiguously by ^{1}H and ^{13}C NMR and high-resolution ESI-MS (Figures S17−S52).

Photoisomerization of SGs. The photoresponsive behavior of **SG1** was studied in an organic solvent by UV−vis absorption and NMR spectroscopy at 298 K (Figure 2). A toluene solution of *cis*-**SG1** (50 μM) has a characteristic strong absorption band at 320−390 nm in the UV−vis spectrum (Figure 2a).

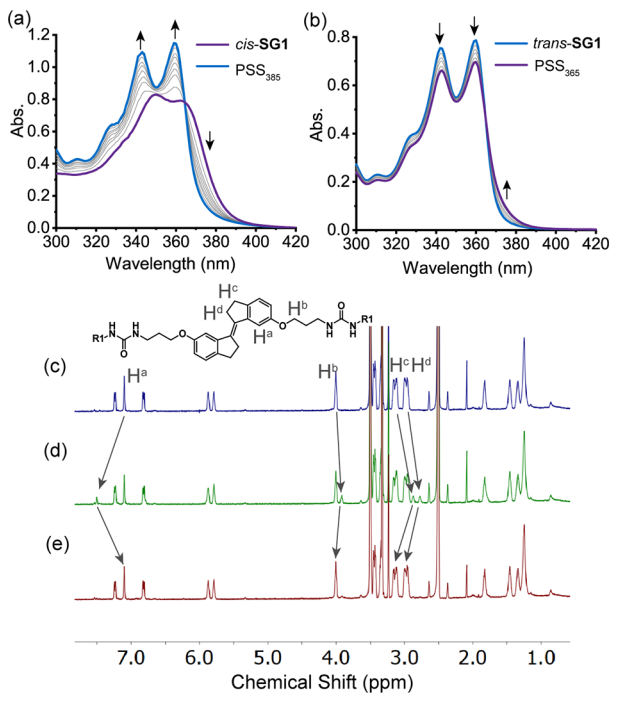

Figure 2. Changes in the UV−vis absorption spectrum (toluene, 298 K) starting from (a) *cis*-**SG1** (50 μM) upon irradiation with 385 nm light for 2 min to PSS_{385} and (b) *trans*-**SG1** (30 μM) upon irradiation with 365 nm light for 1.5 min to PSS_{365}. ^{1}H NMR spectra (DMSO-d_6, 298 K, 400 MHz) of (c) *trans*-**SG1** (4 mM), (d) after irradiation with 365 nm light for 15 min to PSS_{365} (*cis*:*trans* = 33:67), and (e) after subsequent irradiation with 385 nm for 15 min to PSS_{385} (*trans*:*cis* ≥ 99:1).

https://doi.org/10.1021/jacs.1c01802
J. Am. Chem. Soc. 2021, 143, 5990−5997

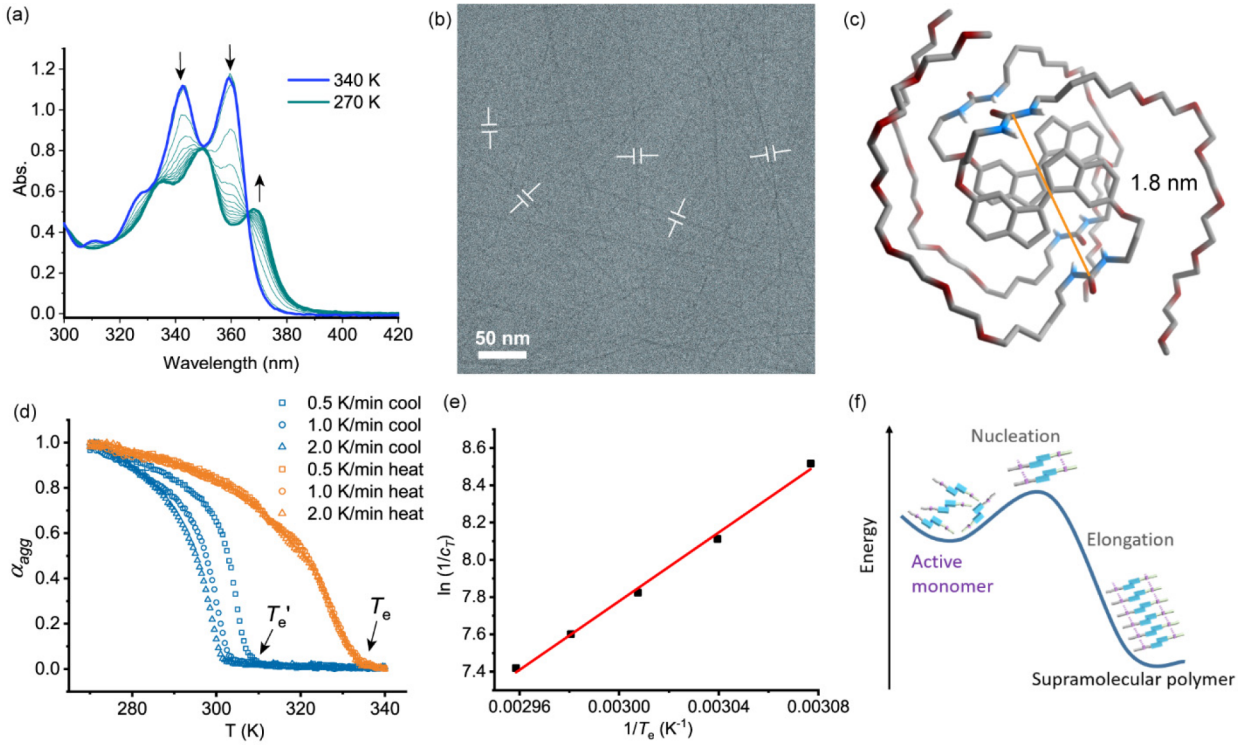

Figure 3. (a) Temperature-dependent changes in the UV−vis absorption spectrum of *trans*-**SG1** (0.4 mM) in toluene during cooling at a rate of 1.0 K/min. (b) Cryo-TEM image of SP-**SG1** formed by *trans*-**SG1** (0.4 mM) after supramolecular polymerization in toluene. (c) Calculated self-assembled structure of *trans*-**SG1** using the ONIOM approach (wB97X-D/def2SVP//wB97X-D/6-31G(d)//UFF). The distance between the urea groups in the dimer is 1.8 nm. (d) Degree of aggregation (α_{agg}, estimated from the UV−vis absorption at 373 nm) of *trans*-**SG1** (c_T = 0.4 mM) as a function of temperature upon cooling and heating at different rates (0.5−2.0 K/min). (e) Natural logarithm of the reciprocal of c_T as a function of the reciprocal of T_e (van't Hoff plot). (f) Schematic illustration of the nucleation−elongation process of *trans*-**SG1**.[32]

Upon 385 nm light irradiation for 2 min, the band at 370−390 nm disappeared with an increase in the absorption maxima at 340 and 360 nm, indicating the conversion of *cis*-**SG1** to *trans*-**SG1**, in accordance with stiff-stilbene photoisomerization.[47,48] A clear isosbestic point at 364 nm confirms the selective unimolecular *cis* to *trans* photoisomerization process. No further spectral change was observed upon prolonged irradiation, indicating that the photostationary state (PSS_{385}) was attained. The resulting solution showed the reverse switching process upon 365 nm light irradiation (Figure S2).

For *trans*-**SG1**, a band appears at 370−390 nm with a decrease in the absorption at 340−360 nm and a clear isosbestic point at 364 nm upon 365 nm light irradiation for 1.5 min, as a consequence of the photoisomerization process from the *trans* to the *cis* isomer (Figure 2b). A spectrum nearly identical with that for *trans*-**SG1** was recovered after subsequent irradiation with 385 nm light for 3 min (Figure S3). This photoisomerization behavior was also demonstrated in DMSO by UV−vis absorption spectroscopy (Figure S4). It was noted that *cis*-**SG1** showed no significant thermally induced switching to *trans*-**SG1** after heating at 323 K for 16 h or at 313 K for 20 h in toluene and DMSO, respectively (Figures S5 and S6), indicating the excellent thermal stability of *cis*-**SG1**.

The ^{1}H NMR spectrum of *trans*-**SG1** in DMSO-d_6 solution (4.0 mM) shows distinctive proton shifts upon photoisomerization. The proton signal of H^a (δ 7.10 ppm) shifts downfield to 7.50 ppm, while H^b, H^c, and H^d shift upfield upon 365 nm light irradiation for 15 min (Figure 2c,d), indicating the conversion from *trans*-**SG1** to *cis*-**SG1**. Integration of the NMR signals established a PSS_{365} ratio of 33:67 (*cis*:*trans*). Subsequent irradiation with 385 nm light for 15 min resulted in the full recovery of the initial ^{1}H NMR spectrum of *trans*-**SG1** with a high PSS_{385} ratio of around 99:1 (*trans*:*cis*, Figure 2e). Essentially identical photoisomerization processes were observed for **SG2** and **SG3** (Figure S7, UV−vis spectra of **SG2** and **SG3**; Figure S8, ^{1}H NMR spectra for **SG2**).

Temperature-Dependent Supramolecular Polymerization in Toluene. To investigate the self-assembly process, changes in the UV−vis absorption spectrum of *trans*-**SG1** (0.4 mM) in toluene were recorded upon cooling from 340 to 270 K at a rate of 1.0 K/min (Figure 3a). The absorption maxima at 343 and 359 nm of *trans*-$\mathbf{SG_1}$ decreased in the cooling process with the formation of a new red-shifted band appearing at around 373 nm, suggesting the formation of well-defined aggregates.[2,34] The presence of a clear isosbestic point at 366 nm and the red-shifted spectra are characteristic for the transition from monomeric *trans*-**SG1** to a supramolecular polymer (SP-**SG1**). To characterize the assembly morphology of SP-**SG1** in toluene, a Volta phase plate was used with cryogenic electron transmission microscopy (cryo-TEM).[57−59] Because the contrast between carbon-based samples and carbon-based solvents is low, the standard method (without a Volta phase plate) of defocusing the image to generate phase contrast loses the resolution to see tiny assemblies in an organic solvent. With the phase plate, phase contrast is generated close to the focus, resulting in a better resolution. To the best of our knowledge, this is the first time a phase plate has been successfully used for nonaqueous samples in cryo-EM. These images show that solutions of SP-**SG1** (0.4 mM)

https://doi.org/10.1021/jacs.1c01802
J. Am. Chem. Soc. 2021, 143, 5990−5997

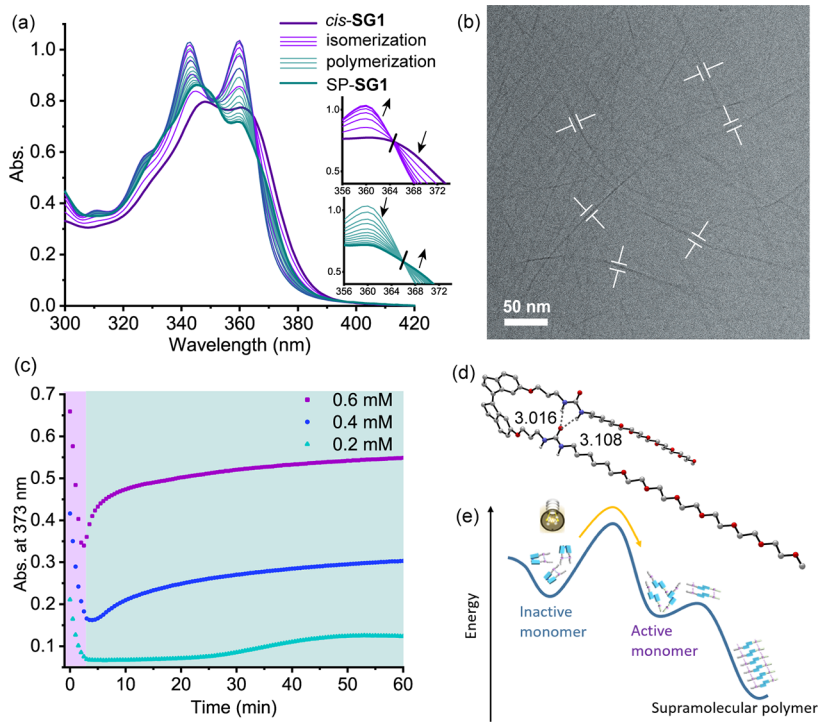

Figure 4. (a) Absorption spectral changes of *cis*-**SG1** (0.4 mM) in toluene at 298 K under 385 nm light irradiation for 2 min and time-dependent changes during supramolecular polymerization. (b) Cryo-TEM image of SP-**SG1** formed by *cis*-**SG1** (0.4 mM) after photoinduced supramolecular polymerization. (c) Plots of the UV−vis absorption at 373 nm as a function of time during the photoinduced polymerization at different total concentrations (c_T). (d) DFT energy minimized structure of *cis*-**SG1** (B3LYP 6-31G+(d,p), IEFPCM toluene). (e) Schematic illustration of the photoinduced supramolecular polymerization of *cis*-**SG1**.[32]

prepared following a procedure identical to that used in the UV−vis studies contained nanofibers with a uniform diameter of 2.5 nm and hundreds of nanometers in length (Figure 3b). The diameter (2.5 nm) of the nanofibers is comparable to the molecular axis of the calculated structure (1.8 nm) using an n-layered integrated molecular orbital and molecular mechanics (ONIOM) approach (Figure 3c), while the intermolecular distance between two monomers was found to be 3.5 Å. The existence of intermolecular hydrogen bonds was further tested by variable-temperature NMR experiments (Figure S12). The proton signals of the ureas (H^1 and H^2 in Figure S12) shift upfield upon heating, with $\Delta\delta/\Delta T = -7.99$ and -8.17 ppb/K, respectively, which is comparable to the shift reported previously for hydrogen-bond-forming urea groups.[68] On the basis of these observations, the obtained supramolecular nanofibers of *trans*-**SG1** are likely built by one-dimensional (1D) stacking of *trans*-**SG1**. This 1D stacking mode is facilitated by the intermolecular hydrogen bonding of the urea moieties in the designed hydrophobic pockets and by the $\pi-\pi$ interactions between the stiff-stilbene core units (Figure 3c).

To identify the polymerization mechanism, we plotted the degree of aggregation (α_{agg}),[23,34] estimated from the absorption at λ = 373 nm, as a function of temperature. Nonsigmoidal curves were observed for *trans*-**SG1** (0.4 mM) upon cooling and heating with a sharp transition at the critical temperatures (T_e' and T_e, respectively, Figure 3d), indicating a nucleation−elongation process.[2,22,24,34,60] Notably, we observed a thermal hysteresis for the heating process with the critical temperature being distinctly higher than for the cooling process (Figure 3d and Figures S9 and S10). For instance, the critical temperature T_e' (cooling process) was 303 at 1.0 K/min, while T_e (heating process) was observed at 333 K (Figure 3d, circles). Furthermore, the value of T_e' was decreased from 307 to 301 K upon increasing the cooling rate from 0.5 to 2.0 K/min (Figure 3d, blue scatters). These data imply that the supramolecular polymerization of *trans*-**SG1** proceeds under kinetic control.[34]

In contrast, we did not observe any notable effect of the heating rate on T_e, indicating that the disassembly process occurs under thermodynamic control (Figure 3d, orange scatters). We fitted the α_{agg} value as a function of temperature with the cooperative model proposed by Meijer and co-workers,[24,34] resulting in an elongation enthalpy value of ΔH_e = −48 kJ mol^{-1} (Figure S10 and Table S1). The degree of aggregation (α_{agg}) at increasing total concentrations (c_T) was recorded as a function of temperature to afford a van't Hoff plot, in which the natural logarithm of the reciprocal of c_T shows a linear relationship with the reciprocal of T_e (Figure 3e). The standard enthalpy ($\Delta H°$) and entropy ($\Delta S°$) associated with the process are −77 kJ mol^{-1} and −165 J mol^{-1} K^{-1}, respectively, resulting in a Gibbs free energy ($\Delta G°$) value of −28 kJ mol^{-1} at 293 K, comparable to that of a known cooperative supramolecular polymerization driven by hydrogen-bond formation.[32] The $\Delta H°$ (−77 kJ mol^{-1}) value obtained from the van't Hoff plot is more negative in comparison to ΔH_e (−48 kJ mol^{-1}), resulting from the cooperative model fitting. This discrepancy might be attributable to the interactions between toluene molecules and monomers[61] that possibly affect the $\Delta H°$ value from the van't Hoff plot but not the ΔH_e value in the cooperative model fitting. The unfavorable entropic term ($-T\Delta S > 0$) parallels the loss of degrees of freedom of the monomers upon polymer formation. Overall, these data suggest that the fibers of *trans*-

https://doi.org/10.1021/jacs.1c01802
J. Am. Chem. Soc. 2021, 143, 5990−5997

Table 1. Solubility and Critical Gelation Concentrations of *trans*-SG1, -SG2, and -SG3 in Different Solvents

trans isomers[a]	water	ethanol	tetrahydrofuran	chloroform	1,4- dioxane	toluene	*p*-xylene	cyclohexane	hexane	1,4-dimethylcyclohexane	cyclooctane	octane
SG1	1.0	s	3.0	s	2.5	1.3	1.3	i	i	i	2.0	i
SG2	2.5	s	7.5	s	5.0	5.0	7.5	i	i	i	7.5	i
SG3	i	gp	gp	1.8	gp	1.0	2.0	i	i	gp	1.8	i

[a]Solubilities are given in units of mg/mL. Abbreviations: i, insoluble during heating; s, soluble at room temperature; gp, gel-like precipitate.

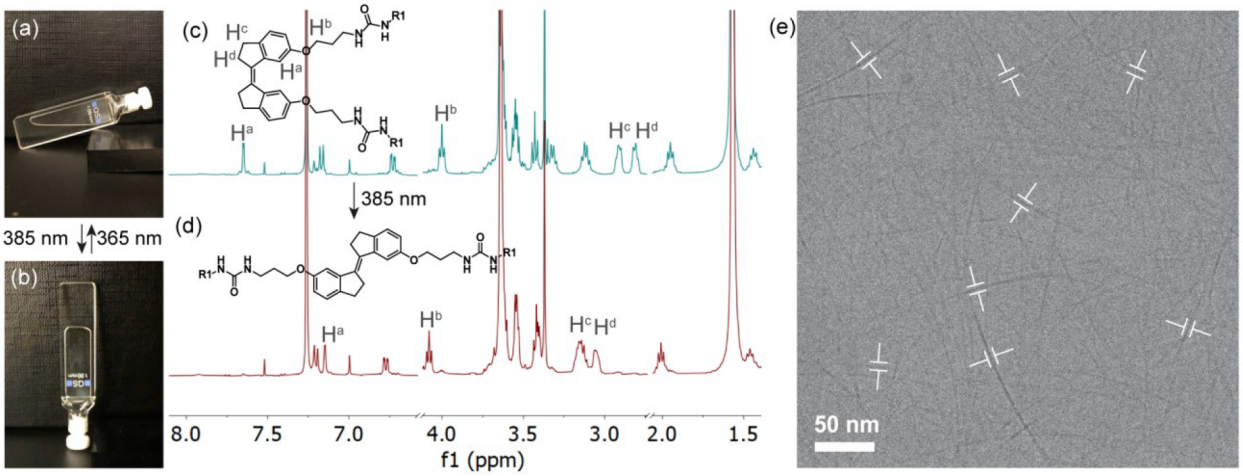

Figure 5. Images of (a) a toluene solution of *cis*-**SG1** (1.5 mg/mL) and (b) the gel obtained after 385 nm irradiation for 3 min and keeping at room temperature for 10 min. ^{1}H NMR spectra of (c) a solution of *cis*-**SG1** and (d) the gel obtained after irradiation with 385 nm light ($CDCl_3$, 298 K, 400 MHz). Samples were characterized after drying from toluene. (e) Cryo-TEM image of the gel formed by *trans*-**SG1** (1.5 mg/mL) in toluene.

SG1 were formed through a cooperative (nucleation−elongation) process.

Photoinduced Supramolecular Polymerization. In stark contrast to *trans*-**SG1**, a toluene solution of *cis*-**SG1** (0.4 mM) did not produce any aggregates observable via cryo-TEM. Moreover, *cis*-**SG1** shows excellent solubility in toluene and is possibly monomeric, as demonstrated by the invariant chemical signal of urea moieties in well-resolved ^{1}H NMR spectra of the compound at different concentrations (Figure S11). To clarify the reason for this difference, we performed FTIR measurements on the toluene solutions of *cis*- and *trans*-**SG1** (Figure S13). *trans*-**SG1** shows a strong vibrational band centered at 3333 cm^{-1}, attributed to hydrogen-bonded N−H in urea moieties.[53,69] *cis*-**SG1** shows a broader band centered at 3396 cm^{-1}, at higher wavenumbers in comparison to the band of *trans*-**SG1** but lower than the free N−H stretching vibration (ca. 3445 cm^{-1}).[70] These results suggest a different hydrogen-bonding pattern for N−H in the two photoisomers. The presence of intramolecular urea hydrogen bonds (revealed by DFT calculations; Figure 4d and Figure S14) might explain the lower ability of the *cis* isomer to form a supramolecular polymer in comparison to the *trans* form. The distances between either nitrogen and the oxygen were 3.016 and 3.108 Å, respectively, in the energy-minimized structure of the *cis* isomer, which is comparable to those observed for other bis-urea derivatives.[38]

Consequently, it should be possible to initiate the supramolecular polymerization upon photoisomerization of the *cis* to the *trans* form (Figure 4e). To prove this concept, we irradiated a toluene solution of *cis*-**SG1** (0.4 mM) with 385 nm light for 3 min to reach PSS. The solution was kept in the dark at 298 K to achieve supramolecular polymerization. The spectral changes upon irradiation revealed a typical *cis* to *trans* photoisomerization in toluene (Figure 4a, purple curves). After irradiation, the spectra remained unchanged for 2 min, indicating no apparent formation of intermediates. The present lag time is associated with the nucleation process.[34] Subsequently, a characteristic increase in absorption around 373 nm with an isosbestic point at 366 nm signaled the formation of aggregates, implying an elongation process (Figure 4a, green curves). Cryo-TEM images showed the presence of fibers with a uniform diameter of 2.5 nm and hundreds of nanometers in length (Figure 4b), confirming the formation of supramolecular polymers. The morphology of the photoinduced supramolecular polymers was identical with those formed by cooling a solution of *trans*-**SG1** (*vide supra*).

To further understand the mechanism of photoinduced supramolecular polymerization, we analyzed the time-resolved UV−vis traces at 373 nm using different concentrations of *cis*-**SG1** in toluene (Figure 4c). With lower concentrations (0.2 and 0.4 mM), the absorption at 373 nm first decreased due to *cis* to *trans* photoisomerization and then increased after a lag time (19 and 2 min, respectively), showing a sigmoidal transition, which is characteristic for an elongation process. These features confirmed that the photoinduced assembly process followed the cooperative (nucleation−elongation) polymerization mechanism.[33,34,62] At the highest concentration (0.6 mM), the lag time is too short to be monitored. The lag time for the polymerization of monomeric *trans* isomers to the supramolecular polymer dramatically decreased with increasing concentration, indicating that the polymerization is under kinetic control,[34] which is in accordance with the study on the temperature-dependent process (*vide supra*). In conclusion, the supramolecular polymerization in this system is successfully triggered by light and these experiments confirm the cooperative (nucleation−elongation) mechanism in toluene.

https://doi.org/10.1021/jacs.1c01802
J. Am. Chem. Soc. 2021, 143, 5990−5997

Gelation Ability and Solvent Screening. Having established the supramolecular polymerization of *trans*-**SG1** in toluene, we continued our investigation toward the development of a supramolecular gel in different solvents. To our delight, *trans*-**SG1** showed excellent gelation ability in a wide range of solvents (Table 1; for more details, see the Supporting Information). As shown in Table 1, the critical gelation concentration (CGC) of *trans*-**SG1** ranges from 1.3 mg/mL in toluene to 3.0 mg/mL in THF. *trans*-**SG1** can hence be categorized as a "supergelator".[38,63,64]

To explore the influence with respect to gelation ability of end groups with different polarity,[54,71] *trans*-**SG2** and *trans*-**SG3** bearing hexaethylene glycol and alkyl chains were also investigated. The CGC values for *trans*-**SG2** are relatively high (from 2.5 to 7.5 mg/mL), which might be attributed to the higher polarity of *trans*-**SG2**.[71] *trans*-**SG3** bearing only an alkyl side chain formed gels in a range of organic solvents. Long fibers with a uniform diameter of 2.5 nm were observed by cryo-TEM in toluene (Figure S15). It should be emphasized that the incorporation of oligoethylene glycol in *trans*-$\mathbf{SG_1}$ and *trans*-**SG2** in contrast to *trans*-**SG3** enables these molecules to gelate not only in organic solvents but also in water. This property could be beneficial for these structures to be applied in the area of smart biomedical materials.[6,11]

***In Situ* Gelation and Gel−Sol Transition Behavior.** As the supramolecular gel is formed by noncovalent interactions, it offers the opportunity to realize macroscopic changes triggered by light.[14−16] A toluene solution of *cis*-**SG1** (1.5 mg/mL) was irradiated with 385 nm light for 3 min in a quartz cuvette at room temperature (Figure 5a). After irradiation, the sample gelated within 10 min (Figure 5b) and cryo-TEM images of the resulting gel showed the presence of fibers (Figure 5e), which are identical to those formed by temperature-dependent and photoinduced supramolecular polymerization (*vide supra*). The solution and gel samples were characterized by ^{1}H NMR in $CDCl_3$ after drying (Figure 5c,d). The signals of *cis*-**SG1** (e.g. H^a 7.64 ppm) had almost disappeared, and a distinct set of signals (e.g. H^a 7.13 ppm) belonging to the *trans* isomer was observed, indicating a *trans*:*cis* ratio at PSS_{385} of 99:1. Upon subsequent irradiation with 365 nm light for 30 min, the gel transformed to a sol again. The lower speed of *trans* to *cis* photoisomerization in the gel state in comparison to that in solution, where the PSS was reached within 15 min, is likely due to the confined space of molecules in the self-assembled fibers.[15,65] To establish the ratio of *trans* to *cis* isomer after the gel to sol process, a gel formed by pure *trans*-**SG1** (1.5 mg/mL) was irradiated to a sol using the same procedure and characterized by ^{1}H NMR in $CDCl_3$ after drying. The *trans*:*cis* ratio in the sol sample was 95:5 (Figure S16), indicating that already a small extent of *trans* to *cis* isomerization caused a gel−sol phase transition in this supramolecular system.[66] In other words, the photo-triggered changes of macroscopic properties of the gel system on the basis of this responsive supramolecular polymer were readily achieved through reversible photoisomerization.

CONCLUSIONS

In conclusion, we developed three stiff-stilbene-based bis-urea monomers, characterized by *cis* isomers acting as inactive monomers, while the *trans* isomers serve as the active monomers for supramolecular polymerization. Thermodynamic studies on the polymerization and depolymerization of the active monomer (*trans*-**SG1**) demonstrated a cooperative supramolecular polymerization in toluene, which was under kinetic control. Due to the high energy barrier of thermal *cis* to *trans* isomerization, this supramolecular polymerization can be precisely triggered by light to form *trans* monomers at room temperature. The photoinduced polymerization follows the nucleation−elongation (cooperative) mechanism. Both processes, temperature-dependent and photoinduced polymerization, were monitored by UV-vis absorption spectroscopy and cryo-TEM with a Volta phase plate. The present study demonstrates precise photocontrol over a supramolecular polymerization. The resulting polymers show a remarkable gelation ability in various organic solvents and reversible changes of macroscopic properties, i.e. a sol−gel transition, which creates opportunities for many potential applications in the field of smart and responsive materials.

ASSOCIATED CONTENT

Supporting Information

The Supporting Information is available free of charge at https://pubs.acs.org/doi/10.1021/jacs.1c01802.

Synthesis, experimental conditions for UV−vis studies, cryo-TEM and computational studies, fitting with the cooperative model, and ^{1}H and ^{13}C NMR spectra (PDF)

Structures of *cis*-**SG1**, *trans*-**SG1**, and *trans*-**SG1** dimer (ZIP)

AUTHOR INFORMATION

Corresponding Author

Ben L. Feringa − *Center for System Chemistry, Stratingh Institute for Chemistry, University of Groningen, 9747 AG Groningen, The Netherlands;* orcid.org/0000-0003-0588-8435; Email: b.l.feringa@rug.nl

Authors

Fan Xu − *Center for System Chemistry, Stratingh Institute for Chemistry, University of Groningen, 9747 AG Groningen, The Netherlands*

Lukas Pfeifer − *Center for System Chemistry, Stratingh Institute for Chemistry, University of Groningen, 9747 AG Groningen, The Netherlands;* orcid.org/0000-0002-8461-3909

Stefano Crespi − *Center for System Chemistry, Stratingh Institute for Chemistry, University of Groningen, 9747 AG Groningen, The Netherlands;* orcid.org/0000-0002-0279-4903

Franco King-Chi Leung − *Center for System Chemistry, Stratingh Institute for Chemistry, University of Groningen, 9747 AG Groningen, The Netherlands;* orcid.org/0000-0003-0895-9307

Marc C. A. Stuart − *Center for System Chemistry, Stratingh Institute for Chemistry, University of Groningen, 9747 AG Groningen, The Netherlands;* orcid.org/0000-0003-0667-6338

Sander J. Wezenberg − *Center for System Chemistry, Stratingh Institute for Chemistry, University of Groningen, 9747 AG Groningen, The Netherlands;* orcid.org/0000-0001-9192-3393

Complete contact information is available at: https://pubs.acs.org/10.1021/jacs.1c01802

Notes

The authors declare no competing financial interest.

https://doi.org/10.1021/jacs.1c01802
J. Am. Chem. Soc. 2021, 143, 5990−5997

■ ACKNOWLEDGMENTS

Financial support from The Netherlands Organization for Scientific Research (NWO-CW), the European Research Council (ERC; advanced Grant No. 694345 to B.L.F.), the Dutch Ministry of Education, Culture and Science (Gravitation program No. 024.001.035), the China Scholarship Council (CSC; No. 201707040064 to F.X.), the Marie Skłodowska-Curie Actions (Individual Fellowship No. 793082 to L.P. and 838280 to S.C.), and the Croucher Foundation (Croucher Startup Allowance to F.K.-C.L.) is acknowledged. We thank Dr. Jan Rheinberger for help with the phase-plate cryo-TEM.

■ REFERENCES

(1) Lehn, J. M. *Supramolecular Chemistry*; Wiley: Weinheim, Germany, 1995.
(2) de Greef, T. F. A.; Smulders, M. M. J.; Wolffs, M.; Schenning, A. P. H. J.; Sijbesma, R. P.; Meijer, E. W. Supramolecular Polymerization. *Chem. Rev.* **2009**, *109*, 5687−5754.
(3) Wehner, M.; Würthner, F. Supramolecular Polymerization through Kinetic Pathway Control and Living Chain Growth. *Nat. Rev. Chem.* **2020**, *4*, 38−53.
(4) Hartlieb, M.; Mansfield, E. D. H.; Perrier, S. A Guide to Supramolecular Polymerizations. *Polym. Chem.* **2020**, *11*, 1083−1110.
(5) Aida, T.; Meijer, E. W.; Stupp, S. I. Functional Supramolecular Polymers. *Science* **2012**, *335*, 813−817.
(6) Krieg, E.; Bastings, M. M. C.; Besenius, P.; Rybtchinski, B. Supramolecular Polymers in Aqueous Media. *Chem. Rev.* **2016**, *116*, 2414−2477.
(7) Würthner, F.; Saha-Möller, C. R.; Fimmel, B.; Ogi, S.; Leowanawat, P.; Schmidt, D. Perylene Bisimide Dye Assemblies as Archetype Functional Supramolecular Materials. *Chem. Rev.* **2016**, *116*, 962−1052.
(8) Kulkarni, C.; Mondal, A. K.; Das, T. K.; Grinbom, G.; Tassinari, F.; Mabesoone, M. F. J.; Meijer, E. W.; Naaman, R. Highly Efficient and Tunable Filtering of Electrons' Spin by Supramolecular Chirality of Nanofiber-Based Materials. *Adv. Mater.* **2020**, *32*, 1904965.
(9) Zhang, Z.; Kim, D. S.; Lin, C. Y.; Zhang, H.; Lammer, A. D.; Lynch, V. M.; Popov, I.; Miljanić, O. S.; Anslyn, E. V.; Sessler, J. L. Expanded Porphyrin-Anion Supramolecular Assemblies: Environmentally Responsive Sensors for Organic Solvents and Anions. *J. Am. Chem. Soc.* **2015**, *137*, 7769−7774.
(10) Dong, R.; Zhou, Y.; Huang, X.; Zhu, X.; Lu, Y.; Shen, J. Functional Supramolecular Polymers for Biomedical Applications. *Adv. Mater.* **2015**, *27*, 498−526.
(11) Yao, S.; Beginn, U.; Gress, T.; Lysetska, M.; Würthner, F. Supramolecular Polymerization and Gel Formation of Bis-(Merocyanine) Dyes Driven by Dipolar Aggregation. *J. Am. Chem. Soc.* **2004**, *126*, 8336−8348.
(12) Yagai, S.; Kinoshita, T.; Higashi, M.; Kishikawa, K.; Nakanishi, T.; Karatsu, T.; Kitamura, A. Diversification of Self-Organized Architectures in Supramolecular Dye Assemblies. *J. Am. Chem. Soc.* **2007**, *129*, 13277−13287.
(13) Hendrikse, S. I. S.; Su, L.; Hogervorst, T. P.; Lafleur, R. P. M.; Lou, X.; van der Marel, G. A.; Codee, J. D. C.; Meijer, E. W. Elucidating the Ordering in Self-Assembled Glycocalyx Mimicking Supramolecular Copolymers in Water. *J. Am. Chem. Soc.* **2019**, *141*, 13877−13886.
(14) Chivers, P. R. A.; Smith, D. K. Shaping and Structuring Supramolecular. *Gels. Nat. Rev. Mater.* **2019**, *4*, 463−478.
(15) Jones, C. D.; Steed, J. W. Gels with Sense: Supramolecular Materials That Respond to Heat, Light and Sound. *Chem. Soc. Rev.* **2016**, *45*, 6546−6596.
(16) Draper, E. R.; Adams, D. J. Low-Molecular-Weight Gels: The State of the Art. *Chem.* **2017**, *3*, 390−410.
(17) Draper, E. R.; Eden, E. G. B.; McDonald, T. O.; Adams, D. J. Spatially Resolved Multicomponent Gels. *Nat. Chem.* **2015**, *7*, 848−852.
(18) de Jong, J. J. D.; Tiemersma-Wegman, T. D.; van Esch, J. H.; Feringa, B. L. Dynamic Chiral Selection and Amplification Using Photoresponsive Organogelators. *J. Am. Chem. Soc.* **2005**, *127*, 13804−13805.
(19) de Jong, J. J. D.; Lucas, L. N.; Kellogg, R. M.; van Esch, J. H.; Feringa, B. L. Reversible Optical Transcription of Supramolecular Chirality into Molecular Chirality. *Science* **2004**, *304*, 278−281.
(20) Li, C.; Iscen, A.; Sai, H.; Sato, K.; Sather, N. A.; Chin, S. M.; Álvarez, Z.; Palmer, L. C.; Schatz, G. C.; Stupp, S. I. Supramolecular−Covalent Hybrid Polymers for Light-Activated Mechanical Actuation. *Nat. Mater.* **2020**, *19*, 900−909.
(21) Chen, J.; Leung, F. K. C.; Stuart, M. C. A.; Kajitani, T.; Fukushima, T.; van der Giessen, E.; Feringa, B. L. Artificial Muscle-like Function from Hierarchical Supramolecular Assembly of Photoresponsive Molecular Motors. *Nat. Chem.* **2018**, *10*, 132−138.
(22) Smulders, M. M. J.; Nieuwenhuizen, M. M. L.; de Greef, T. F. A.; van der Schoot, P.; Schenning, A. P. H. J.; Meijer, E. W. How to Distinguish Isodesmic from Cooperative Supramolecular Polymerisation. *Chem. - Eur. J.* **2010**, *16*, 362−367.
(23) Smulders, M. M. J.; Schenning, A. P. H. J.; Meijer, E. W. Insight into the Mechanisms of Cooperative Self-Assembly: The "Sergeants-and-Soldiers" Principle of Chiral and Achiral C3-Symmetrical Discotic Triamides. *J. Am. Chem. Soc.* **2008**, *130*, 606−611.
(24) Jonkheijm, P.; van der Schoot, P.; Schenning, A. P. H. J.; Meijer, E. W. Probing the Solvent-Assisted Nucleation Pathway in Chemical Self-Assembly. *Science* **2006**, *313*, 80−84.
(25) Kang, J.; Miyajima, D.; Mori, T.; Inoue, Y.; Itoh, Y.; Aida, T. A Rational Strategy for the Realization of Chain-Growth Supramolecular Polymerization. *Science* **2015**, *347*, 646−651.
(26) Gershberg, J.; Fennel, F.; Rehm, T. H.; Lochbrunner, S.; Würthner, F. Anti-Cooperative Supramolecular Polymerization: A New K2-K Model Applied to the Self-Assembly of Perylene Bisimide Dye Proceeding via Well-Defined Hydrogen-Bonded Dimers. *Chem. Sci.* **2016**, *7*, 1729−1737.
(27) Matern, J.; Dorca, Y.; Sánchez, L.; Fernández, G. Revising Complex Supramolecular Polymerization under Kinetic and Thermodynamic Control. *Angew. Chem., Int. Ed.* **2019**, *58*, 16730−16740.
(28) Korevaar, P. A.; George, S. J.; Markvoort, A. J.; Smulders, M. M. J.; Hilbers, P. A. J.; Schenning, A. P. H. J.; de Greef, T. F. A.; Meijer, E. W. Pathway Complexity in Supramolecular Polymerization. *Nature* **2012**, *481*, 492−496.
(29) Fukui, T.; Kawai, S.; Fujinuma, S.; Matsushita, Y.; Yasuda, T.; Sakurai, T.; Seki, S.; Takeuchi, M.; Sugiyasu, K. Control over Differentiation of a Metastable Supramolecular Assembly in One and Two Dimensions. *Nat. Chem.* **2017**, *9*, 493−499.
(30) Wehner, M.; Röhr, M. I. S.; Bühler, M.; Stepanenko, V.; Wagner, W.; Würthner, F. Supramolecular Polymorphism in One-Dimensional Self-Assembly by Kinetic Pathway Control. *J. Am. Chem. Soc.* **2019**, *141*, 6092−6107.
(31) Hirose, T.; Helmich, F.; Meijer, E. W. Photocontrol over Cooperative Porphyrin Self-Assembly with Phenylazopyridine Ligands. *Angew. Chem., Int. Ed.* **2013**, *52*, 304−309.
(32) Endo, M.; Fukui, T.; Jung, S. H.; Yagai, S.; Takeuchi, M.; Sugiyasu, K. Photoregulated Living Supramolecular Polymerization Established by Combining Energy Landscapes of Photoisomerization and Nucleation-Elongation Processes. *J. Am. Chem. Soc.* **2016**, *138*, 14347−14353.
(33) Ogi, S.; Sugiyasu, K.; Manna, S.; Samitsu, S.; Takeuchi, M. Living Supramolecular Polymerization Realized through a Biomimetic Approach. *Nat. Chem.* **2014**, *6*, 188−195.
(34) Ogi, S.; Stepanenko, V.; Sugiyasu, K.; Takeuchi, M.; Würthner, F. Mechanism of Self - Assembly Process and Seeded Supramolecular Polymerization of Perylene Bisimide Organogelator. *J. Am. Chem. Soc.* **2015**, *137*, 3300−3307.
(35) Lutz, J. F.; Lehn, J.-M.; Meijer, E. W.; Matyjaszewski, K. From Precision Polymers to Complex Materials and Systems. *Nat. Rev. Mater.* **2016**, *1*, 16024.
(36) Kitamoto, Y.; Aratsu, K.; Yagai, S. *Photoresponsive Supramolecular Polymers*; Wiley-VCH: Weinheim, Germany, 2019.

https://doi.org/10.1021/jacs.1c01802
J. Am. Chem. Soc. 2021, 143, 5990−5997

(37) Zhang, Q.; Qu, D. H.; Tian, H. Photo-Regulated Supramolecular Polymers: Shining Beyond Disassembly and Reassembly. *Adv. Opt. Mater.* **2019**, *7*, 1900033.
(38) Wezenberg, S. J.; Croisetu, C. M.; Stuart, M. C. A.; Feringa, B. L. Reversible Gel−Sol Photoswitching with an Overcrowded Alkene-Based Bis-Urea Supergelator. *Chem. Sci.* **2016**, *7*, 4341−4346.
(39) Adhikari, B.; Aratsu, K.; Davis, J.; Yagai, S. Photoresponsive Circular Supramolecular Polymers: A Topological Trap and Photo-induced Ring-Opening Elongation. *Angew. Chem., Int. Ed.* **2019**, *58*, 3764−3768.
(40) Nyrkova, I.; Moulin, E.; Armao, J. J.; Maaloum, M.; Heinrich, B.; Rawiso, M.; Niess, F.; Cid, J. J.; Jouault, N.; Buhler, E.; Semenov, A. N.; Giuseppone, N. Supramolecular Self-Assembly and Radical Kinetics in Conducting Self-Replicating Nanowires. *ACS Nano* **2014**, *8* (10), 10111−10124.
(41) Feringa, B. L.; Browne, W. R. *Molecular Switches*; Wiley-VCH: Weinheim, Germany, 2011.
(42) Zhao, Y.-L.; Stoddart, J. F. Azobenzene-Based Light-Responsive Hydrogel System. *Langmuir* **2009**, *25*, 8442−8446.
(43) Iwaso, K.; Takashima, Y.; Harada, A. Fast Response Dry-Type Artificial Molecular Muscles with [C2]Daisy Chains. *Nat. Chem.* **2016**, *8*, 625−632.
(44) Xu, J.-F.; Chen, Y.-Z.; Wu, D.; Wu, L.-Z.; Tung, C.-H.; Yang, Q.-Z Photoresponsive Hydrogen-Bonded Supramolecular Polymers Based on a Stiff Stilbene Unit. *Angew. Chem., Int. Ed.* **2013**, *52*, 9738−9742.
(45) Suzuki, A.; Aratsu, K.; Datta, S.; Shimizu, N.; Takagi, H.; Haruki, R.; Adachi, S.-i; Hollamby, M.; Silly, F.; Yagai, S. Topological Impact on the Kinetic Stability of Supramolecular Polymers. *J. Am. Chem. Soc.* **2019**, *141*, 13196−13202.
(46) Cai, Y.; Guo, Z.; Chen, J.; Li, W.; Zhong, L.; Gao, Y.; Jiang, L.; Chi, L.; Tian, H.; Zhu, W. H. Enabling Light Work in Helical Self-Assembly for Dynamic Amplification of Chirality with Photoreversibility. *J. Am. Chem. Soc.* **2016**, *138*, 2219−2224.
(47) Yan, X.; Xu, J.-F.; Cook, T. R.; Huang, F.; Yang, Q.-Z.; Tung, C.-H.; Stang, P. J. Photoinduced Transformations of Stiff-Stilbene-Based Discrete Metallacycles to Metallosupramolecular Polymers. *Proc. Natl. Acad. Sci. U. S. A.* **2014**, *111*, 8717−8722.
(48) Villarón, D.; Wezenberg, S. J. Stiff-Stilbene Photoswitches: From Fundamental Studies to Emergent Applications. *Angew. Chem., Int. Ed.* **2020**, *59*, 13192−13202.
(49) de Loos, M.; van Esch, J.; Stokroos, I.; Kellogg, R. M.; Feringa, B. L. Remarkable Stabilization of Self-Assembled Organogels by Polymerization. *J. Am. Chem. Soc.* **1997**, *119*, 12675−12676.
(50) de Loos, M.; van Esch, J.; Kellogg, R. M.; Feringa, B. L. Chiral Recognition in Bis-Urea-Based Aggregates and Organogels through Cooperative Interactions. *Angew. Chem., Int. Ed.* **2001**, *40*, 613−616.
(51) Estroff, L.; Hamilton, A. Effective Gelation of Water Using a Series of Bis-urea Dicarboxylic Acids. *Angew. Chem., Int. Ed.* **2000**, *39*, 3447−3450.
(52) Jones, C. D.; Simmons, H. T. D.; Horner, K. E.; Liu, K.; Thompson, R. L.; Steed, J. W. Braiding, Branching and Chiral Amplification of Nanofibres in Supramolecular Gels. *Nat. Chem.* **2019**, *11*, 375−381.
(53) Yanagisawa, Y.; Nan, Y.; Okuro, K.; Aida, T. Mechanically Robust, Readily Repairable Polymers via Tailored Noncovalent Cross-Linking. *Science* **2018**, *359*, 72−76.
(54) Obert, E.; Bellot, M.; Bouteiller, L.; Andrioletti, F.; Lehen-Ferrenbach, C.; Boué, F. Both Water- and Organo-Soluble Supramolecular Polymer Stabilized by Hydrogen-Bonding and Hydrophobic Interactions. *J. Am. Chem. Soc.* **2007**, *129*, 15601−15605.
(55) Pal, A.; Karthikeyan, S.; Sijbesma, R. P. Coexisting Hydrophobic Compartments through Self-Sorting in Rod-like Micelles of Bisurea Bolaamphiphiles. *J. Am. Chem. Soc.* **2010**, *132*, 7842−7843.
(56) Leenders, C. M. A.; Albertazzi, L.; Mes, T.; Koenigs, M. M. E.; Palmans, A. R. A.; Meijer, E. W. Supramolecular Polymerization in Water Harnessing Both Hydrophobic Effects and Hydrogen Bond Formation. *Chem. Commun.* **2013**, *49*, 1963−1965.
(57) Danev, R.; Buijsse, B.; Khoshouei, M.; Plitzko, J. M.; Baumeister, W. Volta Potential Phase Plate for In-Focus Phase Contrast Transmission Electron Microscopy. *Proc. Natl. Acad. Sci. U. S. A.* **2014**, *111*, 15635−15640.
(58) Lafleur, R. P. M.; Herziger, S.; Schoenmakers, S. M. C.; Keizer, A. D. A.; Jahzerah, J.; Thota, B. N. S.; Su, L.; Bomans, P. H. H.; Sommerdijk, N. A. J. M.; Palmans, A. R. A.; Haag, R.; Friedrich, H.; Böttcher, C.; Meijer, E. W. Supramolecular Double Helices from Small C3-Symmetrical Molecules Aggregated in Water. *J. Am. Chem. Soc.* **2020**, *142*, 17644−17652.
(59) Franken, L. E.; Grünewald, K.; Boekema, E. J.; Stuart, M. C. A. A Technical Introduction to Transmission Electron Microscopy for Soft-Matter: Imaging, Possibilities, Choices, and Technical Developments. *Small* **2020**, *16*, 1906198.
(60) Aratsu, K.; Takeya, R.; Pauw, B. R.; Hollamby, M. J.; Kitamoto, Y.; Shimizu, N.; Takagi, H.; Haruki, R.; Adachi, S.-i; Yagai, S. Supramolecular Copolymerization Driven by Integrative Self-Sorting of Hydrogen-Bonded Rosettes. *Nat. Commun.* **2020**, *11*, 1−12.
(61) Isobe, A.; Prabhu, D. D.; Datta, S.; Aizawa, T.; Yagai, S. Effect of an Aromatic Solvent on Hydrogen-Bond-Directed Supramolecular Polymerization Leading to Distinct Topologies. *Chem. - Eur. J.* **2020**, *26*, 8997−9004.
(62) Lohr, A.; Würthner, F. Evolution of Homochiral Helical Dye Assemblies: Involvement of Autocatalysis in the "Majority-Rules" Effect. *Angew. Chem., Int. Ed.* **2008**, *47*, 1232−1236.
(63) Qi, Z.; Wu, C.; Malo de Molina, P.; Sun, H.; Schulz, A.; Griesinger, C.; Gradzielski, M.; Haag, R.; Ansorge-Schumacher, M. B.; Schalley, C. A. Fibrous Networks with Incorporated Macrocycles: A Chiral Stimuli-Responsive Supramolecular Supergelator and Its Application to Biocatalysis in Organic Media. *Chem. - Eur. J.* **2013**, *19*, 10150−10159.
(64) Wang, T.; Yu, X.; Li, Y.; Ren, J.; Zhen, X. Robust, Self-Healing, and Multistimuli-Responsive Supergelator for the Visual Recognition and Separation of Short-Chain Cycloalkanes and Alkanes. *ACS Appl. Mater. Interfaces* **2017**, *9*, 13666−13675.
(65) Velema, W. A.; Stuart, M. C. A.; Szymanski, W.; Feringa, B. L. Light-Triggered Self-Assembly of a Dichromonyl Compound in Water. *Chem. Commun.* **2013**, *49*, 5001−5003.
(66) Weyandt, E.; ter Huurne, G. M.; Vantomme, G.; Markvoort, A. J.; Palmans, A. R. A.; Meijer, E. W. Photodynamic Control of the Chain Length in Supramolecular Polymers: Switching an Intercalator into a Chain Capper. *J. Am. Chem. Soc.* **2020**, *142*, 6295−6303.
(67) Albertazzi, L.; van der Zwaag, D.; Leenders, C. M. A.; Fitzner, R.; van der Hofstad, R. W.; Meijer, E. W. Probing Exchange Pathways in One-Dimensional Aggregates with Super-Resolution Microscopy. *Science* **2014**, *344*, 491−495.
(68) Li, X.; Mignard, N.; Taha, M.; et al. Thermoreversible Supramolecular Networks from Poly (Trimethylene Carbonate) Synthesized by Condensation with Triuret and Tetrauret. *Macromolecules* **2019**, *52*, 6585−6599.
(69) Ayzac, V.; Sallembien, Q.; Raynal, M.; Isare, B.; Jestin, J.; Bouteiller, L. A. Competing Hydrogen Bonding Pattern to Yield a Thermo-Thickening Supramolecular Polymer. *Angew. Chem., Int. Ed.* **2019**, *58*, 13849−13853.
(70) Teo, L.; Chen, C.; Kuo, J. Fourier Transform Infrared Spectroscopy Study on Effects of Temperature on Hydrogen Bonding in Amine-Containing Polyurethanes and Poly (Urethane-Urea)S. *Macromolecules* **1997**, *30*, 1793−1799.
(71) Wilder, E. A.; Hall, C. K.; Khan, S. A.; Spontak, R. J. Effects of Composition and Matrix Polarity on Network Development in Organogels of Poly(Ethylene Glycol) and Dibenzylidene Sorbitol. *Langmuir* **2003**, *19*, 6004−6013.

https://doi.org/10.1021/jacs.1c01802
J. Am. Chem. Soc. 2021, 143, 5990−5997